Pure Appl. Geophys.

https://doi.org/10.1007/s00024-021-02801-3

Pure and Applied Geophysics

Basement and Structure Near the Southwestern Margin of the Lower Benue Trough Between, and Including, the Anambra Basin and Afikpo Syncline, as Derived from Aeromagnetic and Gravity Data

Mukaila Abdullahi[1] and Raj Kumar[2]

Abstract—We present depth estimates and structural information, using aeromagnetic and gravity data, relating to the basement near the southwestern margin of the lower Benue trough between, and including, the Anambra basin and Afikpo syncline. The basement depth is calculated on the basis of the scaling spectral method, Euler deconvolution, and source parameter imaging (SPI) applied to gridded aeromagnetic data and 2D gravity modeling across the three main tectonic features (i.e., Anambra basin, Abakaliki anticlinorium, and Afikpo basin/syncline). We interpreted basement depths between 8.4 and 9.1 km within the Anambra basin, 3.1 and 9.8 km within the Abakaliki anticlinorium, and 3.8–8.5 km within the Afikpo basin/syncline. The magnetic basement depths estimated from the three methods applied on the aeromagnetic data are in good agreement with each other and that provided by the 2D gravity model which produced a reliable picture of the basement relief in the region. We also mapped and interpreted magnetic lineaments/faults in the region. Three well-defined magnetic lineaments/faults (NE–SW, ENE–WSW, and WNW–ESE) correlate very closely with the trends of geological structures of the Pan-African plate which predated the compressional folds and faults within the Cretaceous sediments and strike-slip movements during the separation of Africa and South America.

Keywords: Lower Benue trough, aeromagnetic and gravity data, basements, scaling spectral method, Euler method, SPI, 2D gravity modeling.

1. Introduction

Gravity and magnetic data have proven cost-effective in the interpretation of basement relief and geological structures/features (Adighije, 1981; Ali et al., 2014; Ofoegbu, 1985; Salem et al., 2014). They both reflect the variations in the physical properties (density and/or susceptibility) of the subsurface crust, and in the present case of sediments and the underlying basement rocks. Gravity and magnetic data/methods have been essential for the interpretation of geological/tectonic features such as strike-slip faults and regional discontinuity, dykes, and basement relief, which in most cases are difficult to interpret from a seismic perspective (Ali et al., 2017). Mapping of magnetic basement and/or sedimentary basin thickness is very paramount in geophysical prospecting for mineral or petroleum exploration (Telford et al., 1998). Mapping the subsurface provides critical knowledge relating to the basement relief of a region.

Methods of magnetic basement estimation have involved the wavenumber domain (Nabighian et al., 2005; Salem et al., 2014; Spector & Grant, 1970), structural indices (Hood, 1965; Reid et al., 1990; Reid & Thurston, 2014), and the local wavenumber (Salem & Smith, 2005; Thurston & Smith, 1997). The method utilizing the wavenumber domain can be applied in the case for either randomly and uncorrelated distribution of magnetic sources, as outlined in Spector and Grant's (1970) method, or as in the case of scaling/fractal (i.e., randomly and correlated) distribution of magnetic sources (Bansal & Dimri, 2010; Kumar et al., 2018; Maus & Dimri, 1996). Depth estimation using the Euler deconvolution approach requires that the choice of the structural index be consistent with the geometry of the structure whose depth is being estimated, along with definition of suitable window sizes, otherwise precise locations of geological structures and depths are likely to be incorrect (Reid & Thurston, 2014). The local

[1] Physics Unit, Department of Science Laboratory Technology, Modibbo Adama University, P.M.B. 2076, Yola, Nigeria. E-mail: mukailaa.agp@mautech.edu.ng

[2] Shillong Geophysical Research Centre (Indian Institute of Geomagnetism Mumbai), Shillong 793005, India.

Published online: 19 July 2021

wavenumber approach as in source parameter imaging (SPI) utilizes the first-order local wavenumber to give the horizontal distribution of magnetic sources as well as the depth solutions for a given real model such as a contact, dike, or cylinder (Salem & Smith, 2005).

Interpretations of gravity anomalies associated with sedimentary basins have been undertaken in several studies (Ali et al., 2014; Rao et al., 1993). Interpretation of gravity anomalies from the perspective of a 2D modeling approach is very effective, especially for irregularly shaped bodies (Talwani et al., 1959). This approach has an advantage of addressing the issue of multiple geological structures within the crust.

The study area (Fig. 1) includes the Anambra basin, Abakaliki anticlinorium, and Afikpo syncline. The Anambra basin is an integral part of the lower Benue trough (Figs. 2 and 3), a subdivision of the Nigeria Benue trough, an intracontinental basin that formed an integral part of the west and central African Rift System, whereas the Afikpo syncline is also a basin that is synclinal in nature (Tokam et al., 2010). A southwest to northeast cross section along the entire Benue trough, extending from the Atlantic Ocean to the Chad basin, is displayed in Fig. 2. Stratigraphically, the sediments of the Anambra basin range from Campanian to Paleocene in age (Fig. 3). The development of the region resulted from the separation of Africa from South America and the opening of the Atlantic Ocean and Gulf of Guinea between the late Jurassic and the early Cretaceous (Jassen et al., 1995; King, 1950; Ofoegbu & Onuoha, 1991). A uniqueness of the region, among others, is the folded Cretaceous sedimentary rocks (Carter et al., 1963). Even though folding in the region is

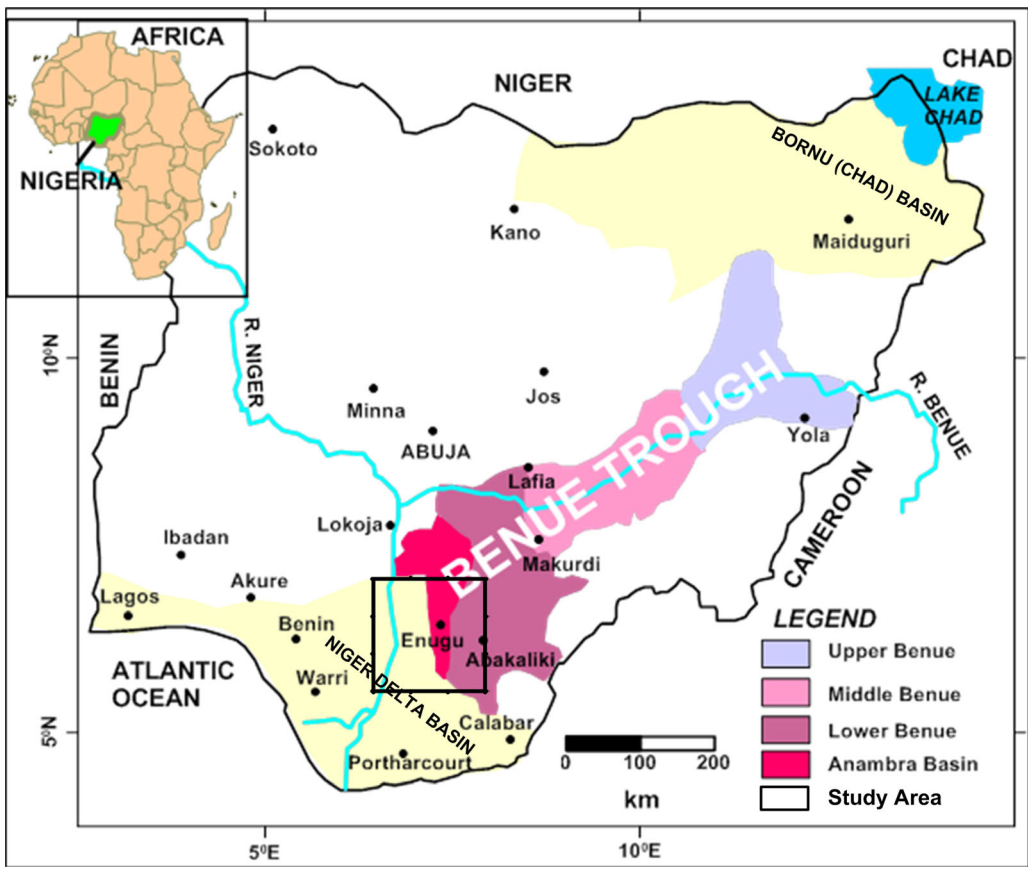

Figure 1
Simplified geological map of Nigeria, showing the study region (modified after Ogunmola et al., 2016)

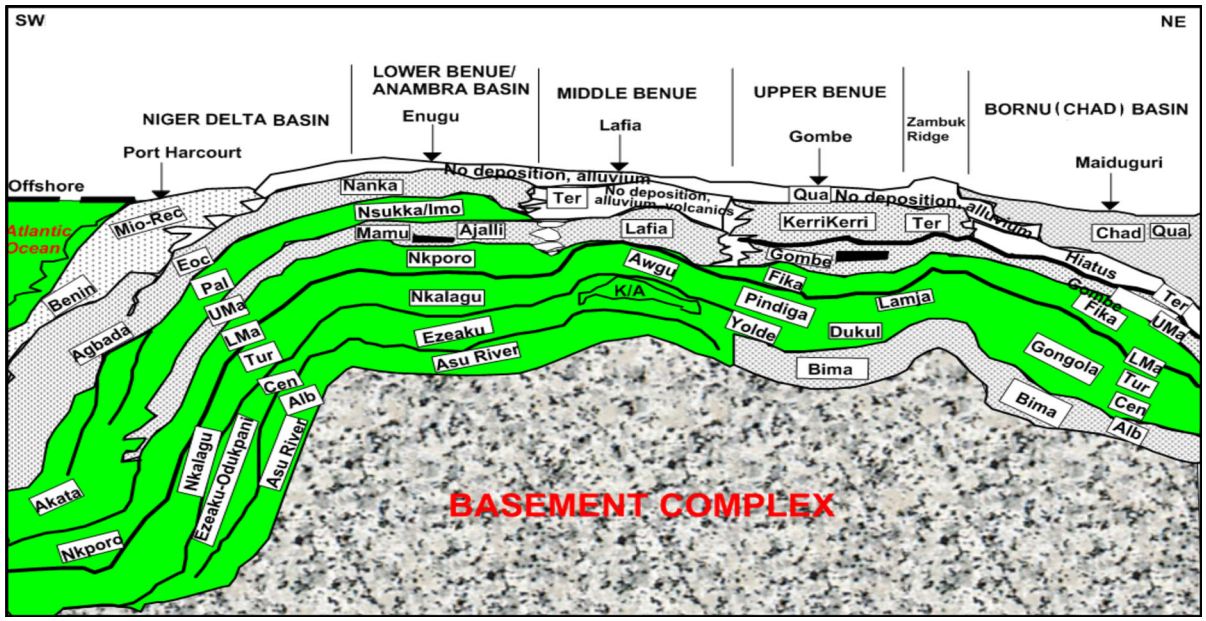

Figure 2
The idealized northeast–southwest stratigraphic cross section across the Chad basin-Benue trough-Niger Delta basin showing different formations and their respective ages. The cross section was modified from Obaje (2009)

generally dated as Santonian (Cratchley & Jones, 1965), others are of the opinion that some of the folds are Maastrichtian (Adighije, 1981; Agagu & Adighije, 1983; Ajayi & Ajakaiye, 1981, 1986).

In the present study, we have calculated basements using the scaling spectral method for aeromagnetic data, 3D Euler deconvolution for aeromagnetic data, SPI for aeromagnetic data, and 2D forward modeling for gravity data in an attempt to investigate basement structural trends for the trapping of hydrocarbons and hosting of other economic mineral resources in the region.

2. *Geological Setting*

The first cycle of sedimentation within the region of the study is the marine Albian Asu river group (Fig. 2) inter-fingered with mafic igneous rocks (Abdullahi & Singh, 2018; Cratchley & Jones, 1965; Obaje, 2009; Ofoegbu, 1985; Agagu & Adighije, 1983; Ojoh, 1992; Onwuemesi, 1997; Uzuakpunwa, 1974). The Asu river group is found around the area of Abakaliki (Fig. 1). The Asu river group comprises shales, limestones, and sandstone intercalations with an estimated thickness of about 2.0 km (Adighije, 1981). The next cycle of sedimentation in the region is the Ezeaku shale/Makurdi sandstones/Ajali sandstones whose relationship to the Asu river group is unconformable (Agagu & Adighije, 1983). The age of the Ezeaku/Makurdi formation is Turonian whose deposition is thought to have begun in the Upper Cenomanian (Ofoegbu, 1985). Overlying the Ezeaku/Makurdi formation is the Late Turonian to Coniacian marine-type fossiliferous grey bluish shale, limestone, and calcareous sandstone Nkalagu formation (Offodile, 1976; Ofoegbu, 1985). The Campanian Nkporo formation in the lower Benue consisting of shales and mudstones unconformably overlies the Nkalagu formation (Fig. 3) and is overlain by the lower coal measures/Mamu formation consisting mainly of sandstones, carbonaceous shales, sandy shales, and local coal seams (Cratchley & Jones, 1965; Kogbe, 1981; Obaje, 2009; Offodile, 1976; Ofoegbu, 1985). The Ajali formation conformably overlies the Mamu formation. Another cycle of sedimentation, regarded to be the latest in the region, is the sequence of Late Maastrichtian-Early Paleocene

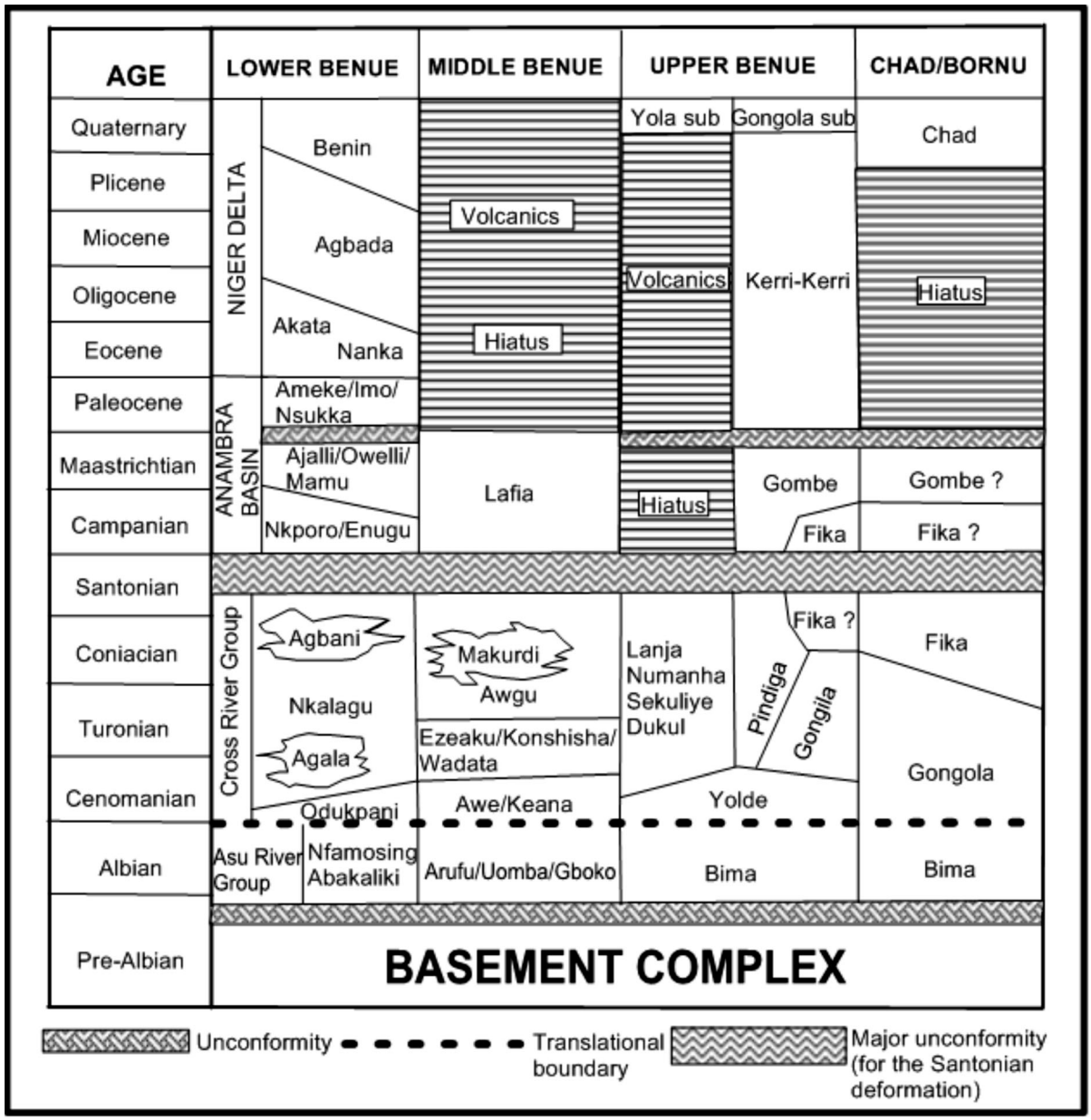

Figure 3
The stratigraphic successions in the section of Nigeria's Chad basin and Benue trough (i.e. lower Benue, middle Benue, and upper Benue). The figure is modified after Obaje (2009)

carbonaceous shales and coal seams of Ameke/Imo/Nsukka formations (Figs. 4, 5). The Nsukka and Imo formations represent the major formations found within the Anambra basin. The Imo shale contains a large amount of organic matter which could be interpreted as a source of hydrocarbon for the area just north of the Niger Delta basin (Obaje, 2009).

There is report of igneous activity underneath the trough which is grouped into the younger and the older intrusive (Anudu et al., 2014; Carter et al., 1963; Cratchley & Jones, 1965; Ofoegbu,

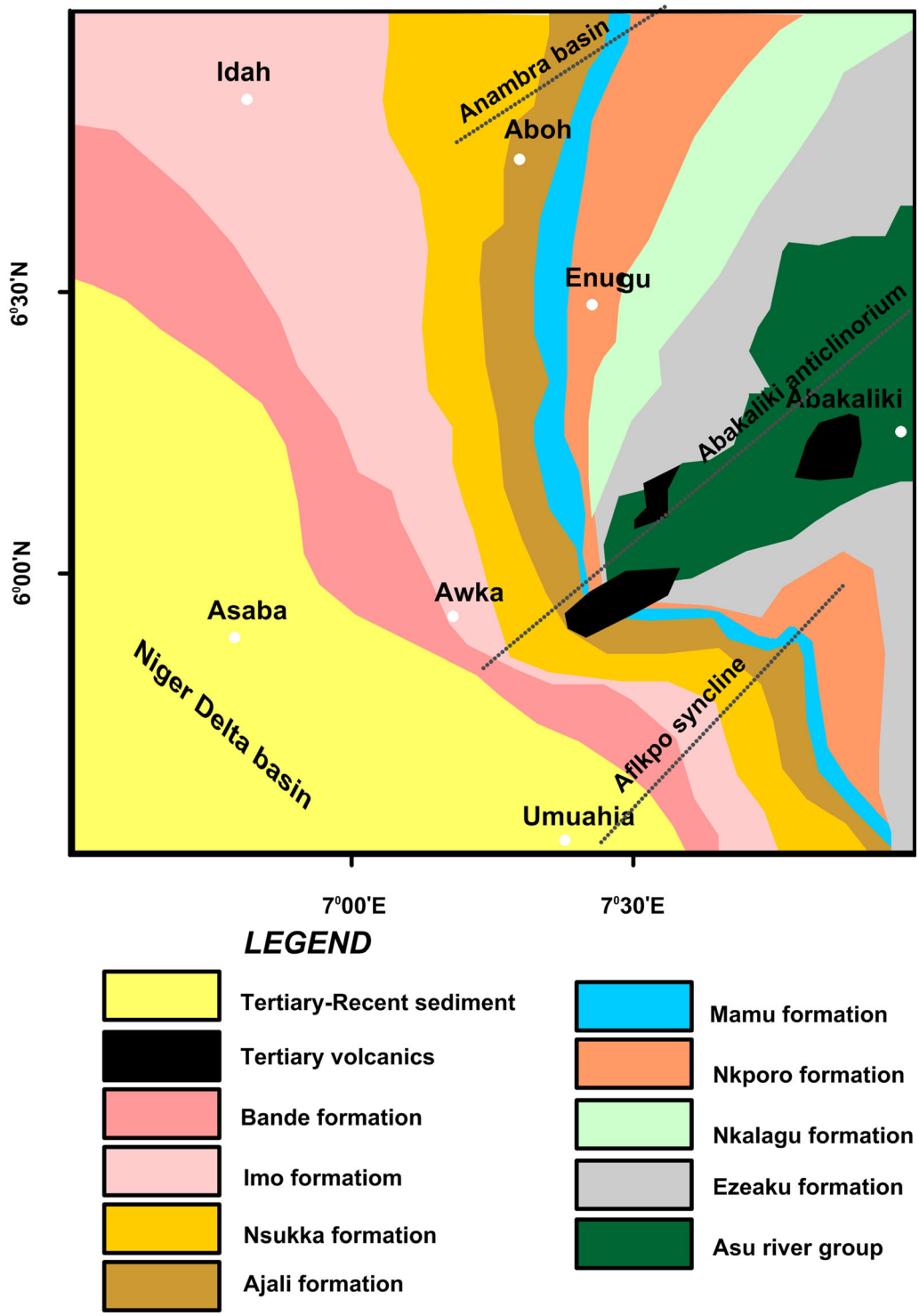

Figure 4
Geological map of the study region (Anambra basin and environs). The three important tectonic structures (i.e. the Abakaliki anticlinorium, Afikpo syncline, and the Anambra basin) are plotted (modified after Ogungbesan & Adedosu, 2019)

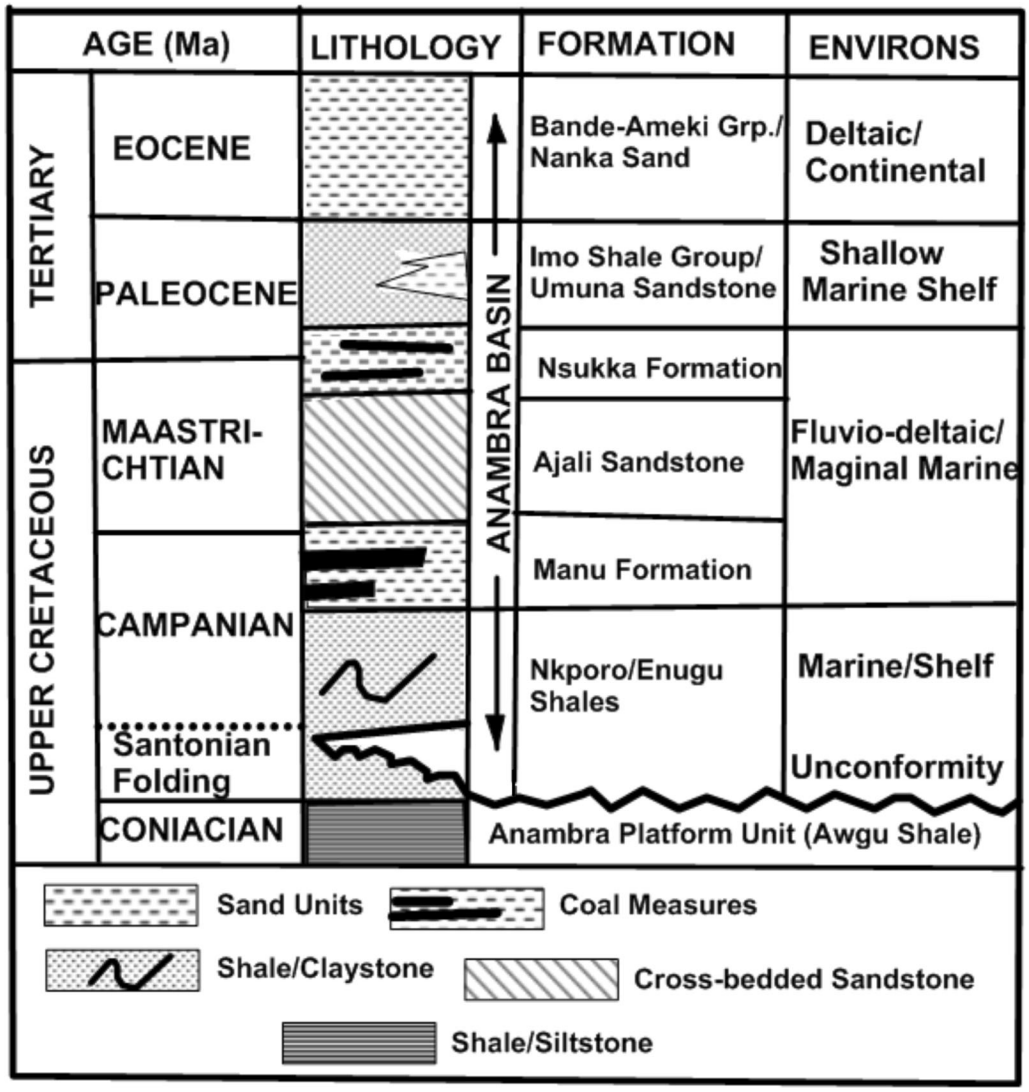

Figure 5
Stratigraphy and depositional environments of sedimentary infill within the Anambra basin (modified after Agagu & Adighije, 1983; Ogungbesan & Adedosu, 2019)

1984, 1985; Ofoegbu & Onuoha, 1991). The older group includes the granites of basic and diabasic types associated with dyke-like bodies (Maluski et al., 1995). They represent the granitic evolution in which all states of granitization and magmatism are displayed (Maluski et al., 1995; Ofoegbu, 1984, 1985). They show similarity in foliation, which makes them hard to identify from their metamorphosed series. The older granites have intruded the basement complex at different time right during the evolution of the gneisses, and the amount of crystallization varies based upon age (Carter et al., 1963).

The younger igneous activity within the region is mainly basalts and pegmatites, although diorites, dolerites, and some syenites also occur as a small cones, plugs, lavas sheets, and tuffs of different sizes (Adighije, 1981; Ajayi & Ajakaiye, 1981; Cratchley & Jones, 1965). Pegmatite dykes composed of microcline and quartz are found within the vicinity of older granites (Ofoegbu, 1985). They are mostly only

a few meters in thickness, but could be put together to form a single large body (Ajayi & Ajakaiye, 1981).

3. Data and Methods

3.1. Aeromagnetic Data

More recent high-resolution aeromagnetic data covering the entire country are available from the Nigerian Geological Survey Agency (NGSA) as acquired between 2005 and 2009 and interpreted by Reford and Paterson (2010). Part of the region under study has been interpreted in terms of its magnetic basement and crustal thermal structure (Abdullahi & Kumar, 2020; Abdullahi et al., 2019a, 2019b). In most cases, the traverse line spacing for the acquisition of the high-resolution aeromagnetic data is 500 m with 2-km control line spacing and elevation of 80 m (Abdullahi et al., 2019b). It is therefore very apparent that for a small area of coverage, one could obtain numerous observation points of the data which may not be suitable for the application of some techniques (e.g., in the present case, the Euler deconvolution and SPI methods among others).

The magnetic anomaly map presented (Fig. 6) is derived from the data that was used to investigate the magnetic basement and Curie depth of the region (Onwuemesi, 1997). The data were acquired under the supervision of NGSA and cover the areas of the Anambra basin, Abakaliki anticlinorium, and the Afikpo syncline. The survey was conducted at an elevation of about 500 m above the ground level with a line spacing of 2 km along lines oriented NW–SE and NE–SW. Data were collected with an optically pumped cesium-type split-beam sensor magnetometer having a sensitivity of 0.001 nT that recorded data every 0.1 s. The data were then corrected for edge effects and diurnal variations, subsequently levelled, and the geomagnetic gradient was removed using an appropriate International geomagnetic reference field. Finally, a regional component of the magnetic field was removed from the derived map by fitting and removing linear surfaces to produce a gridded residual component at a 2-km grid interval which is considered to represent a signature of the geology of the region (Onwuemesi, 1997).

3.2. Estimation of Depth to Magnetic Basements

Many techniques and methods have been developed for depth interpretation of magnetic data (Blakely, 1996; Nabighian et al., 2005; Spector & Grant, 1970). The scaling spectral method is a modification of the Spector and Grant (1970) method whereby top depths to magnetic sources and a new parameter called the scaling exponent (β) are simultaneously calculated (Kumar et al., 2018; Maus & Dimri, 1996). The top depths are commonly interpreted in terms of various geological features in the subsurface of the earth (Kumar et al., 2018). Other semi-automated depth estimation methods include, for example, the Euler deconvolution method (Reid et al., 1990) and SPI (Thurston & Smith, 1997) based on the location of the sources of the model parameters.

3.2.1 Scaling Spectral Method

The scaling spectral method has been designed on the basis of randomly correlating homogeneously ensemble blocks of magnetic sources where depth to top of the magnetic body (d_t) and scaling exponent (β) are simultaneously calculated by inverting spectra (Kumar et al., 2018) as:

$$P(w) = cw^{-\beta}e^{-2|w|d_t} \tag{1}$$

where c is a constant that depends on the properties of the magnetic sources, $P(w)$ is the power spectrum of magnetization, and w is the radial wavenumber in rad/km.

Scaling exponent (β) is a parameter introduced in the Spector and Grant (1970) method to test for heterogeneity for randomly correlating the distribution of magnetic sources inside the earth (Abdullahi et al., 2019b; Kumar et al., 2018). This parameter is small for a large depth of investigation and vice versa for randomly correlating magnetic sources, and a scaling exponent value of zero (0) means uncorrelated distribution of magnetic sources (Pilkington & Todoeschuk, 1993). The values of scaling exponent (β) can therefore be used to interpret a tectonically unstable (complex) region.

Depth estimation using the spectral approach depends on the size of the selected window. For

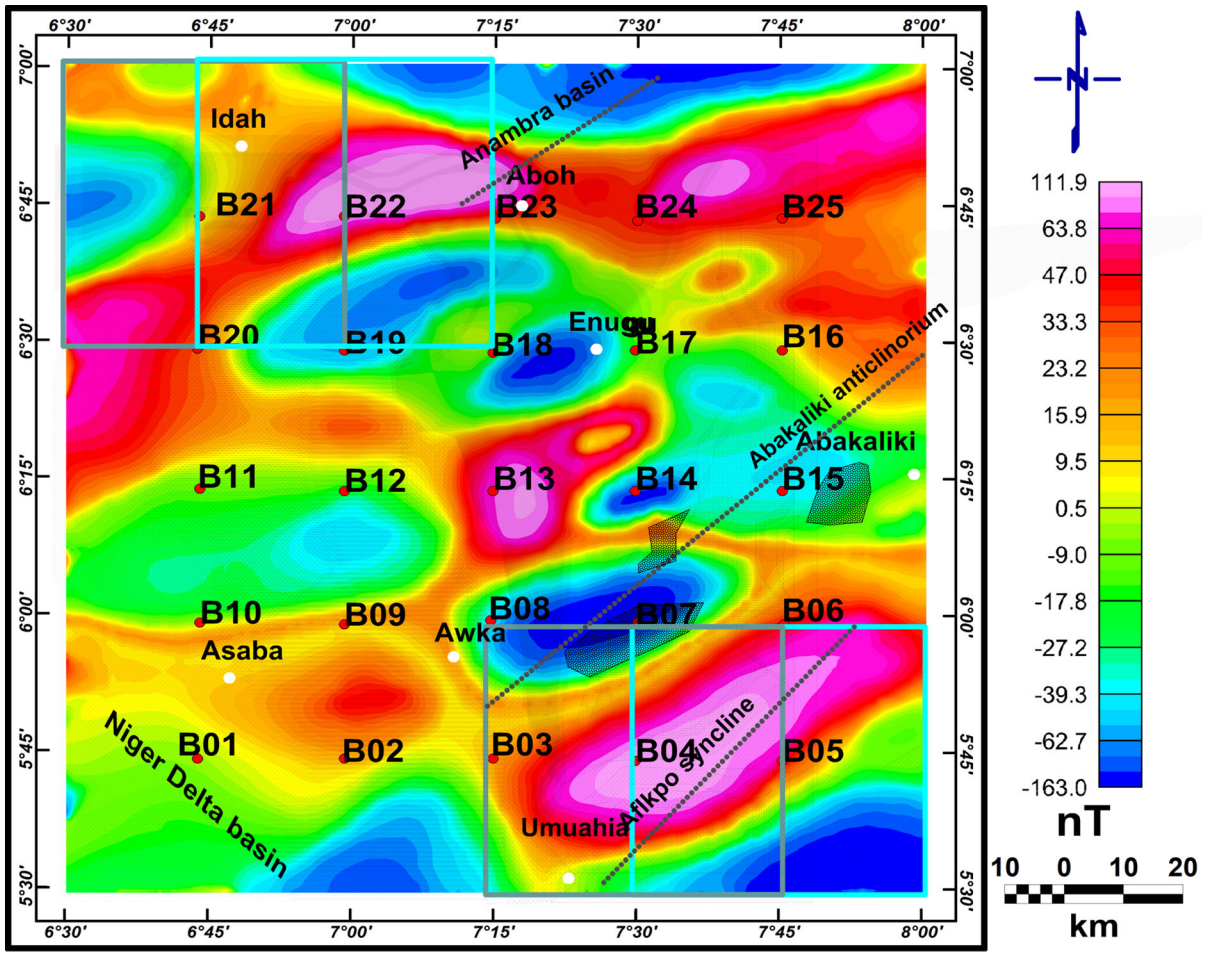

Figure 6
Total magnetic intensity (TMI) anomaly map of aeromagnetic data of the study area. Shown on the map are the central points of the subregions (in red cross) labeled B01, B02, …, B25. The window size selection (55 km × 55 km) and the 50% overlapping in cyan and oceanic green squares as are shown on the SE and NW edges of the anomaly map. The three tectonic structures in the region and the geology are also superimposed on the map. Note the zones of tertiary volcanics along the axis of the Abakaliki anticlinorium

reliable depth calculations, at least five times the expected depth is considered appropriate (Kumar et al., 2020). In the present study, we prepared 25 subregions (blocks) of 55 km × 55 km with 50% overlap from the TMI aeromagnetic anomaly (Fig. 6). Each block has been processed separately for the simultaneous calculation of the depths and scaling exponent values. Presented in Fig. 7 is an example of one of the power spectra generated in block B03. The results for the total of 25 subregions are as shown in Table 1.

3.2.2 *Euler Deconvolution*

The Euler deconvolution method has been a very rapid tool of choice for the interpretation of potential field data, perhaps because of its easy implementation (Keating, 1998; Mushayandebvu et al., 2001; Reid et al., 1990; Thompson, 1982). The method is based on the homogeneity equation (Reid et al., 1990; Thompson, 1982):

$$(x - x_0)\frac{\partial F}{\partial x} + (y - y_0)\frac{\partial F}{\partial y}(z - z_0)\frac{\partial F}{\partial z} = N(B - F) \tag{2}$$

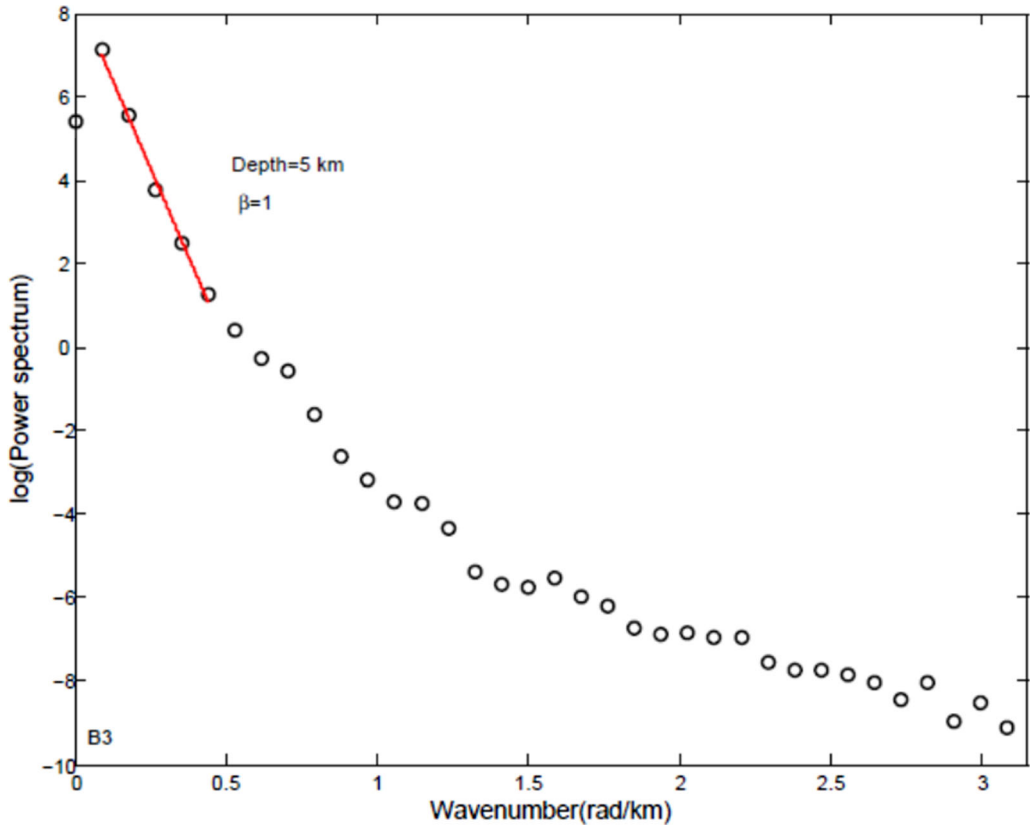

Figure 7
Example of one of the 25 power spectra generated from block B03 for the simultaneous estimation of depths (km) and the scaling exponent values

where x, y, z denote the coordinates of plane of observation. x_0, y_0, and z_0 denote the source locations. The capital letter B is the background constant of the magnetic field F, and N is the structural index. This relationship relates the magnetic field and the components of its gradient to the location and depth of sources using a specified chosen structural index (SI = N) (Ravat, 1996; Thompson, 1982). The numeric choice of the SI is very important, as it is directly linked to the geological body and must be compatible with the geometry of the body. The optimum structural index for a geological body is usually identified by the structural index that produces the tightest clustering of solutions (Reid, 1995). For magnetic data, there are four options of structural indices solutions. A structural index of 3 is consistent with a spherical structure beneath the Earth's surface. Pipe/cylinder/thin bed/fault-like structures have a structural index of 2; a structural index of 1 corresponds to a body having the shape of a thin sheet, whereas for an infinite contact/fault the structural index is 0 (Reid & Thurstone, 2014). Reduction of magnetic data to the pole before the application of Euler deconvolution is immaterial, because the method can directly reproduce the precise location of magnetic sources without the data having been reduced to the magnetic pole (Reid et al., 1990).

The total magnetic intensity (TMI) anomaly map is used for the Euler deconvolution. The stable Euler solution of the aeromagnetic data over the area is calculated using a structural index of 0 and a window size of 10 km × 10 km. Moreover, the choice of a structural index of 0 is because the Euler solution corresponding to infinite contacts/faults is directly associated with all geological bodies, no matter what their size and shape are, and since faults are of prime

Table 1

Result of estimates of the magnetic basement (km) and scaling exponent values from the scaling spectral method

Block subregions	Magnetic depths (km)	Scaling exponent values
B01	2.0	1.0
B02	3.0	1.0
B03	5.0	1.0
B04	2.0	2.0
B05	2.0	2.0
B06	8.0	0.0
B07	7.0	0.0
B08	4.0	0.9
B09	8.0	0.0
B10	4.0	0.8
B11	7.0	0.0
B12	5.0	0.2
B13	3.0	1.0
B14	3.0	0.8
B15	2.0	2.0
B16	0.4	4.0
B17	5.0	0.3
B18	7.0	0.06
B19	6.0	0.5
B20	7.0	0.0
B21	5.0	0.5
B22	9.0	0.0
B23	8.0	0.02
B24	1.0	2.0
B25	3.0	2.0

importance in controlling structures that could act as a trap for hydrocarbon accumulations in the present geological setting. Results for these values are shown in Fig. 8, in which calculated depths to the tops of magnetic sources range between 1.3 and 9.1 km.

3.2.3 *Source Parameter Imaging (SPI) and Structural Elements*

The SPI method is a semi-automated technique for the estimation of magnetic source depth (z) defined as the inverse of the peaks of the horizontal local wavenumber ($k_{\max}$) (Thurston & Smith, 1997):

$$\text{Depth}(z) = \frac{n+1}{k_{\max}} \tag{3}$$

where n is a parameter analogous to the geological structural index in Euler deconvolution.

For a contact model with $n = 0$, Eq. (3) can be rewritten as:

$$\text{Depth}(z) = \frac{1}{k_{\max}}, \tag{4}$$

where $k_{\max}$ represents the horizontal local wavenumber of the observed magnetic field (F), which can be calculated in terms of the horizontal and vertical derivatives of the field (Philips et al., 2007) as:

$$k_{\max} = \frac{1}{\left(\frac{\partial F}{\partial x}\right)^2 + \left(\frac{\partial F}{\partial y}\right)^2 + \left(\frac{\partial F}{\partial z}\right)^2} \times \left(\frac{\partial F}{\partial x}\frac{\partial^2 F}{\partial x \partial z} + \frac{\partial F}{\partial y}\frac{\partial^2 F}{\partial y \partial z} + \frac{\partial F}{\partial z}\frac{\partial^2 F}{\partial z^2}\right) \tag{5}$$

The SPI method has an advantage over the Euler deconvolution in that it does not depend on the selection of window size.

The SPI technique has been applied to the aeromagnetic data, and the depths and distribution of magnetic sources are as shown in Fig. 9. The calculated depths are in the range between 0.6 and 9.8 km.

Superimposed on this map (Fig. 9) are magnetic lineaments interpreted from the results of Euler deconvolution shown in Fig. 8. Most of these lineaments trend either NE–SW, ENE–WSW, WNW–ESE, or W–E, with a few generally shorter lineaments trending NW–SE. Most of the lineaments were interpreted in an earlier study of high-resolution aeromagnetic data of the lower Benue region (Abdullahi et al., 2019a). This present study, therefore, finds correlations of these lineaments with those interpreted from other regions of the Benue trough.

3.3. *Gravity Data*

The Bouguer gravity field of the study area (Fig. 10) represents one of the data sets interpreted by Adighije (1981) for the general crustal architecture of the region and later interpreted by Abdullahi and Singh (2018) for basement geology. In the present study, the data are used to derive the structural geology below subsurface. These data were collected during gravity surveys of the Benue trough in the period 1975–1977, which completed measurements at 600 different stations in the region. The data used are digitized from Adighije (1981) and then sorted and

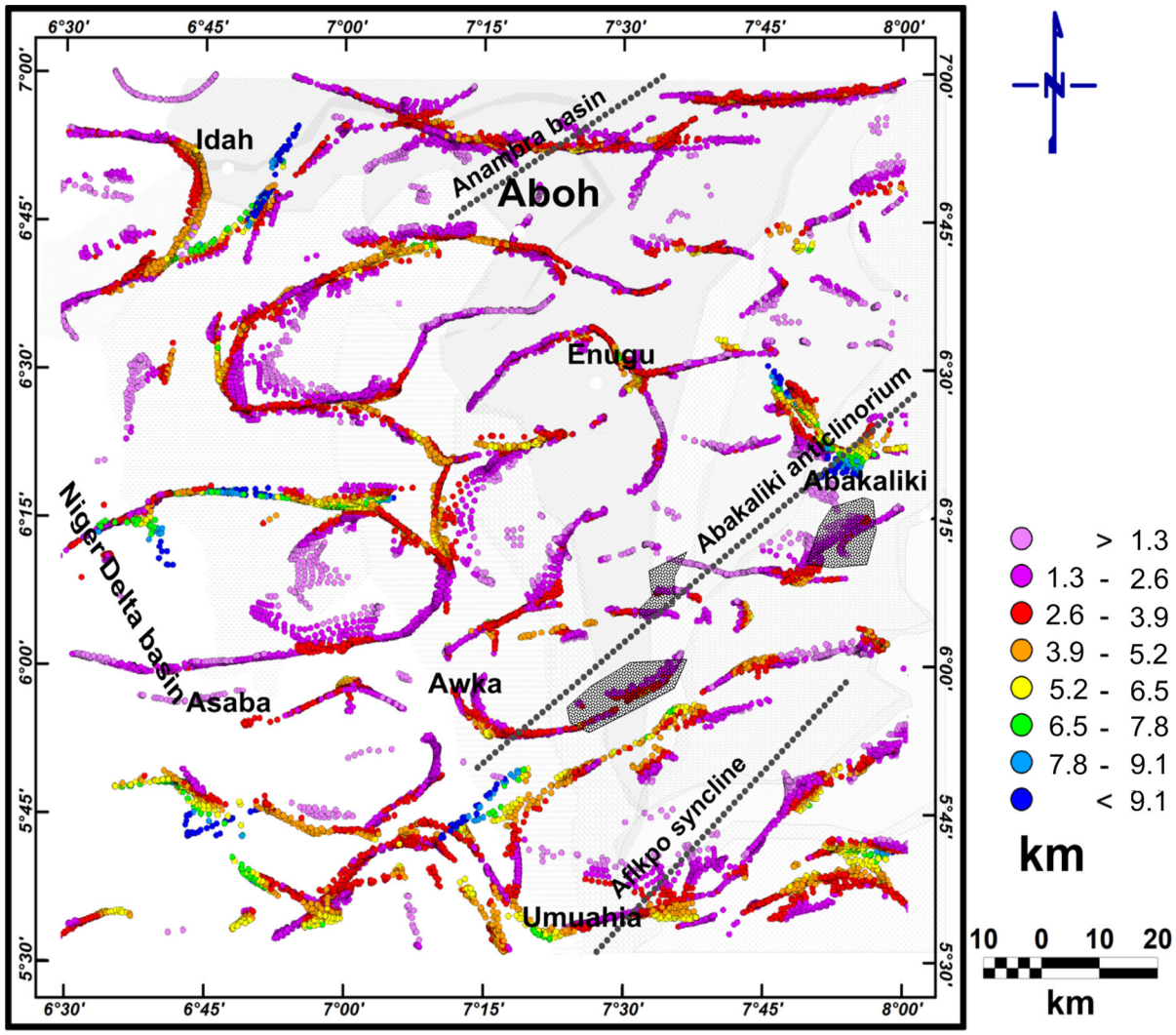

Figure 8
Results of the 3D Euler deconvolution for contacts. Structural index (SI = 0.0); window size (WS = 10 km × 10 km). Depths (km) of 1.3–9.1 km are shown. Note the zones of tertiary volcanics along the axis of the Abakaliki anticlinorium

re-gridded at an interval of 2 km to produce the map displayed in Fig. 10. The three principal geological structures in the region are superimposed on this map. It is clear that the prominent central gravity high correlates closely with the axis of the Abakaliki anticlinorium as interpreted with observed gravity (Abdullahi & Singh, 2018; Adighije, 1981; Agagu & Adighije, 1983). The Anambra basin and the Afikpo syncline coincide with noticeable gravity lows near the north-central margin and southeastern corner of the area, respectively (Fig. 10). The thick black line oriented NW–SE (AB) on the figure is the profile line for 2D forward modeling.

3.4. 2D Forward Modeling of Gravity Anomaly

A 2D gravity model has been interpreted using the commercial software GM-SYS developed by Geosoft and based on the algorithm of Talwani et al. (1959) and Won and Bevis (1987). The software permits modifications to the geometries and densities of geological units in the process of achieving a match

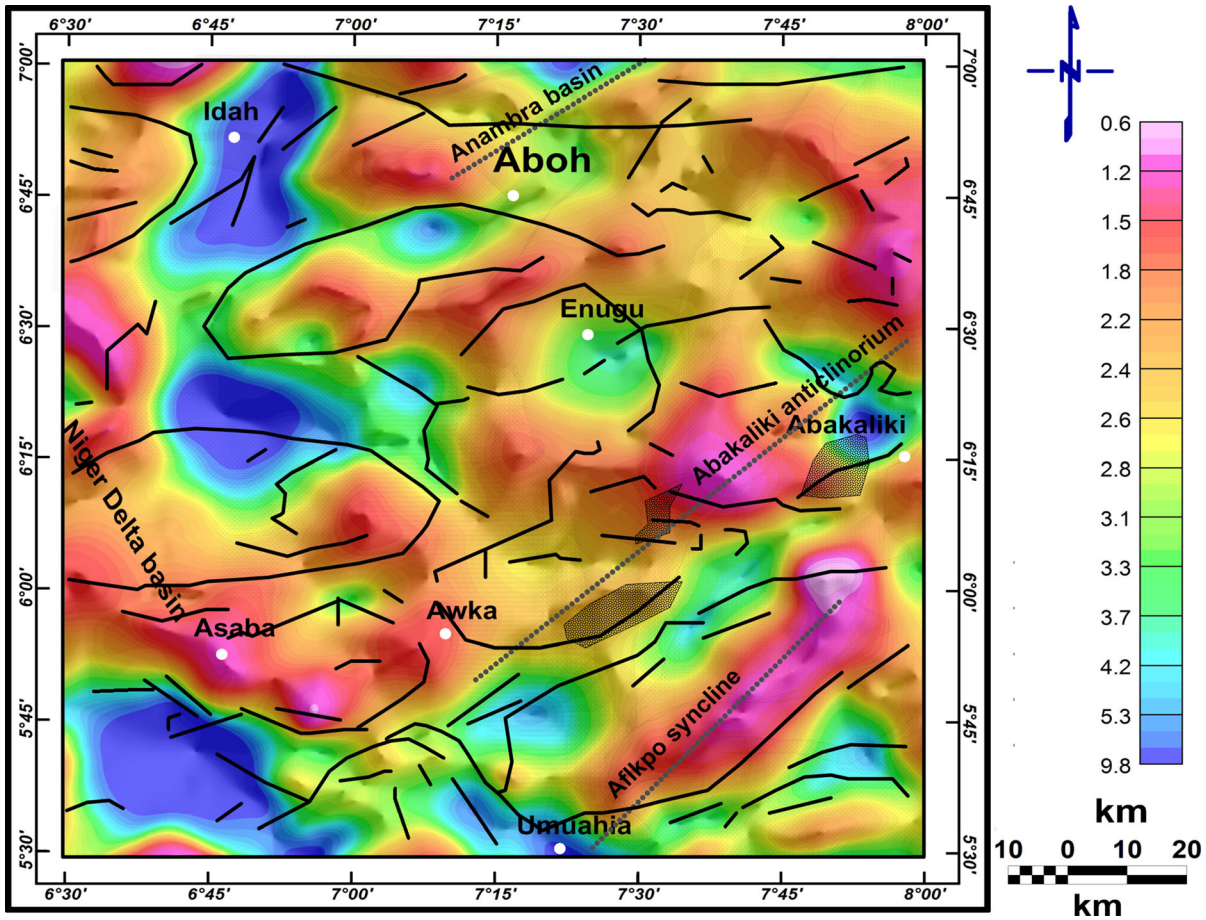

Figure 9
Source parameter imaging (SPI) results (contact model with structural index $n = 0.0$) showing the distribution and contacts between geologic structures within depths (km) of 0.6–9.8 km. The superimposed black lines are interpreted basement structures from Fig. 8. Note the zones of tertiary volcanics along the axis of the Abakaliki anticlinorium

to the observed gravity profile. The 2D forward modeling of the gravity data has been constrained partly by depths derived from the present analysis of aeromagnetic data and other published gravity models in the region (Abdullahi & Singh, 2018; Adighije, 1981). The only selected gravity profile cuts across the Abakaliki anticlinorium, Afikpo syncline/basin, and Anambra basin (Fig. 10). On the profile, two important positive gravity anomalies are clearly shown. The broad, smooth gravity high with an estimated amplitude of about 4.4 mGal correlates with the Anambra basin. This could be due to the high-density sedimentary rocks in the lower half of the basin sequence. The adjacent principal gravity high near the southeast end of the model is of significantly higher amplitude, about 13.2 mGal, and has been modelled as a mafic intrusion (2.76 g cm^{-3}), tentatively identified as syenite (Abdullahi & Singh, 2018; Ajayi & Ajakaiye, 1981). This prominent gravity high coincides with a zone of a relatively negative magnetic anomaly (Fig. 6). This could suggest that the intrusions are weakly magnetic. It is also interesting to note that in the southeastern low gravity (nearly −20 mGal) where we expected to see basin thickening, we observed interpreted sedimentary cover of only 3.8 km. This may be because of the uplifted basement followed probably by a very thick Cretaceous sedimentary rock of the Asu river group in the lower portion of the basin. This area coincided with a magnetic high,

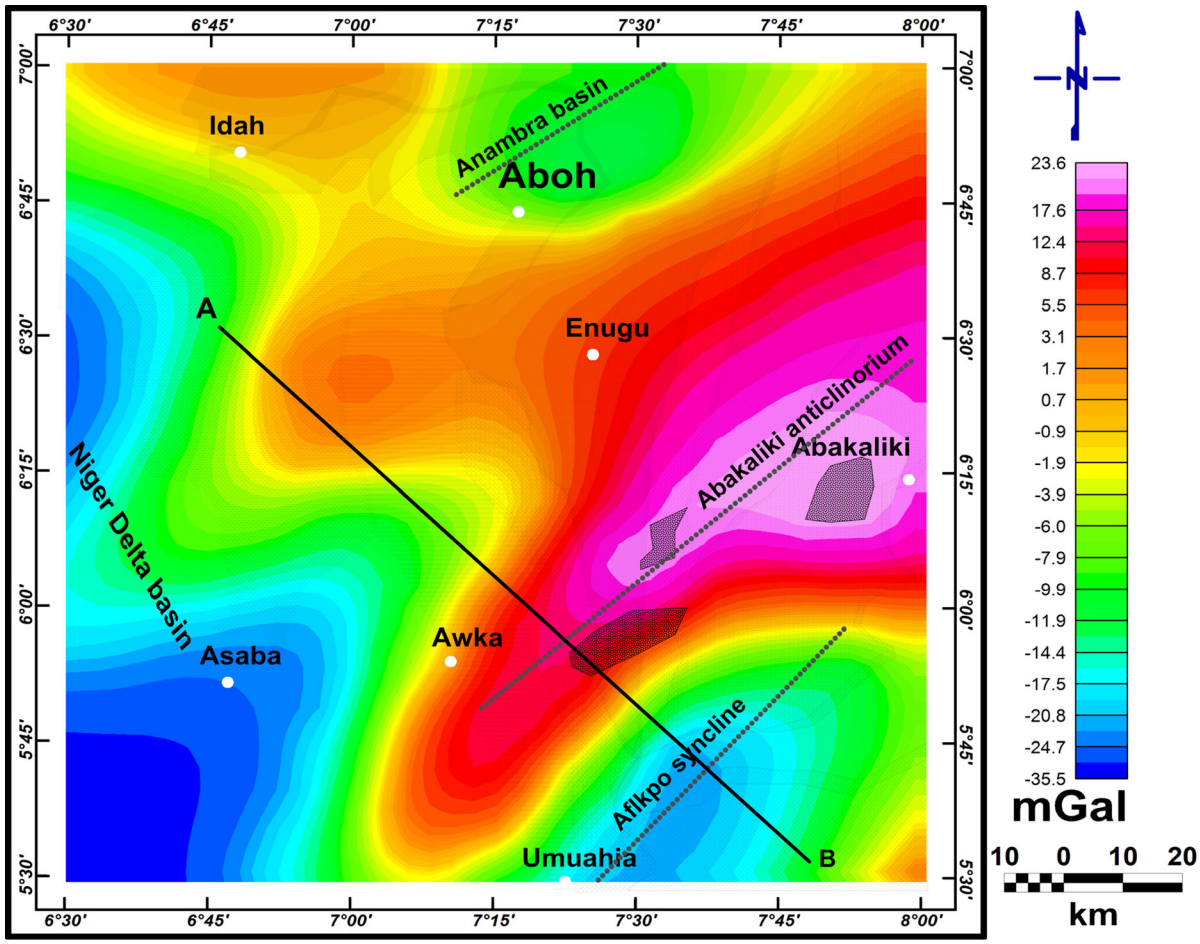

Figure 10
Gravity anomaly map of the study area with locations of the Anambra basin, Abakaliki anticlinorium, and Afikpo syncline delineated. The grey areas in the figure coincide with the zones of tertiary volcanics along the axis of the Abakaliki anticlinorium

which could be interpreted as a highly magnetized zone.

4. *Results and Discussion*

The results of the three separate sets of depth estimates applied to the aeromagnetic data and presented here are equally important. The study area includes the three major tectonic structures in the region“ Anambra basin, Abakaliki anticlinorium, and Afikpo syncline.

The scaling spectral method suggests that the maximum depth of the magnetic basement is 9.0 km at the southwestern end of the Anambra basin (Fig. 11). This is consistent with the sedimentary thickness of 8.4–9.0 km reported for the basin by Agagu and Adighije (1983). A shallow magnetic basement at a depth of 0.4 km is also interpreted in the region. This is located near the northeastern part of the Abakaliki anticlinorium where the anticline is believed to be more tightly folded (Ofoegbu, 1984). On the other hand, at the southwestern end of the Abakaliki anticlinorium, the magnetic basement is interpreted to be at a depth of 4.0 km very close to Awka, and at a depth of 7.0 km about 20 km east of Awka. Zero scaling exponent values are calculated within some blocks: B6 depth of 8.0 km northeast of

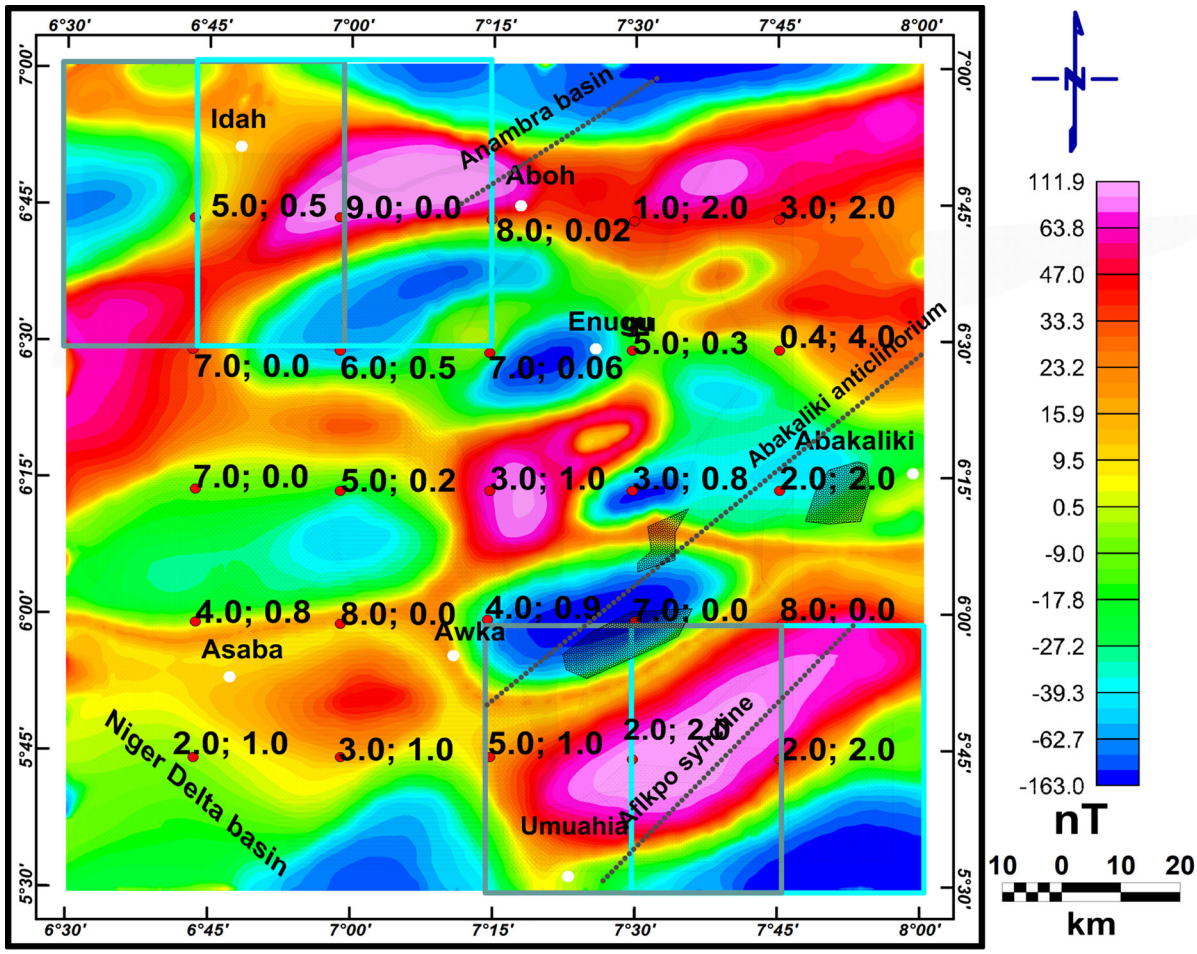

Figure 11

Results of the depths (km) and scaling exponent values from the application of the scaling spectral method superimposed on the TMI anomaly map of the study area. The window size selection (55 km × 55 km) and the 50% overlapping in cyan and oceanic green squares are as shown on the SE and NW edges of the anomaly map. Note the zones of tertiary volcanics along the axis of the Abakaliki anticlinorium

the Afikpo syncline, B7 depth of 7.0 km southwest of the Abakaliki anticlinorium, B22 depth of 9.0 km northeast of the Anambra basin, and also in blocks B9, B11, and B20 at depths of 8.0 km, 7.0 km, and 7.0 km, respectively. This indicates the uncorrelated distribution of magnetic sources within the region. As a general note, the values of the scaling exponent as calculated are not always correlated with the calculated depths, which indicates the complex nature of the region.

The Euler method and SPI present most similar depth results and distribution of sources. This could be because the two methods actually depend on similar hypotheses with little difference in practical application. Results from both Euler and SPI methods delineate infinite contacts between geological structures in the area and predict that the magnetic basement around the Anambra basin lies at depths of 9.1 km and 9.8 km near Idah, respectively, whereas a depth of 9.0 km is calculated using the scaling spectral method towards the southwestern edge of the Anambra basin itself (Table 2). The mean maximum basement depth calculated by the SPI is 700 m greater than the mean derived from the Euler method. The model interpreted from the gravity profile indicates that the Anambra basin has a maximum sedimentary thickness of around 8.4 km. Over the Abakaliki anticlinorium, the maximum magnetic

Table 2

Maximum basement depths in the major tectonics calculated using the scaling spectral method, Euler deconvolution, source parameter imaging (SPI) of aeromagnetic data, and 2D forward modeling of gravity data

Structure	Scaling spectral method of aeromagnetic data (km)	Euler method of aeromagnetic data (km)	SPI method of aeromagnetic data (km)	2D forward modeling of gravity data (km)
Anambra basin	9.0	9.1	9.8	8.4
Abakaliki anticlinorium	5.0	9.1	9.8	3.1
Afikpo basin	7.8	8.5	8.0	3.8

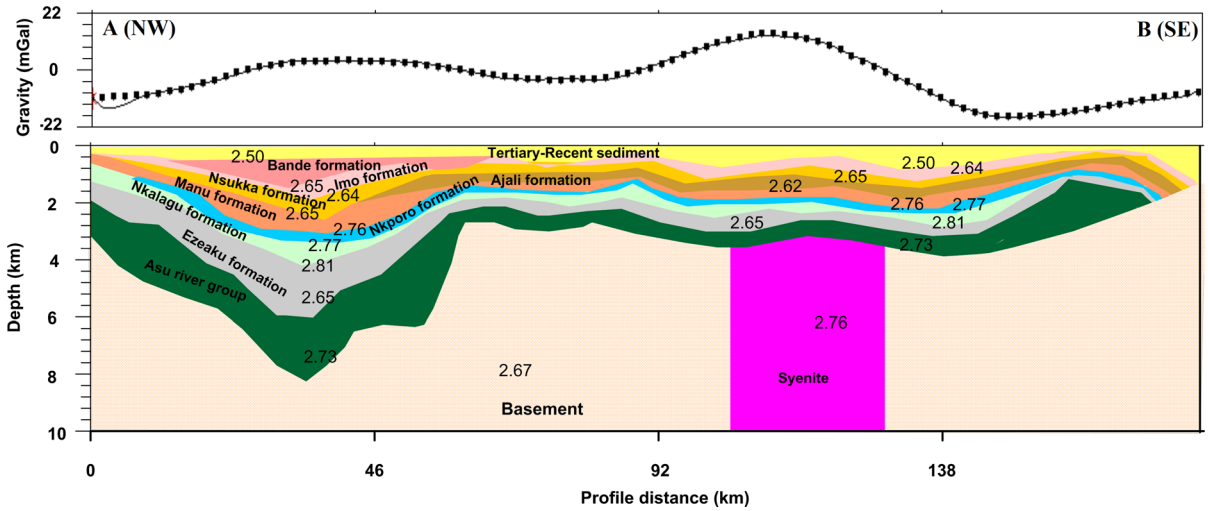

Figure 12
2D model of the gravity anomaly along the profile line AB (NW–SE). In the sedimentary successions overlying the Precambrian basement, densities of individual horizons are indicated in g/cm^3. The solid profile line represents observed gravity values in mGal, and the dotted profile represents the calculated values

basement of 9.1 km and 9.8 km is also calculated from the northeastern and southwestern edge of the anticlinorium structure using the Euler and SPI methods, respectively. Using the scaling spectral method, a maximum magnetic basement of 5.0 km is calculated for the southwestern edge of the anticlinorium, and only 2.0 km is calculated for the northeastern edge around Abakaliki town. In contrast, from the 2D gravity modeling, we recorded a maximum sedimentary basement of 3.1 km over a modeled and interpreted syenite (2.76 g cm^{-3}) structure near the southwestern edge of the Abakaliki anticlinorium (Table 2). In the Afikpo synclinal basin structure, southeast of the structure, depths of around 7.8 km and 8.5 km are calculated using Euler and SPI methods, respectively. The result from the scaling spectral method indicates a magnetic basement of 8.0 km. A sedimentary basement of 3.8 km is calculated from the perspective of the 2D gravity model.

Moreover, the 2D modeled gravity profile has outlined the different geological formations/geological sections in the region of study. The Asu river group (with density of 2.73 g cm^{-3}) and several other Cretaceous sedimentary horizons overlie the Precambrian basement (2.67 g cm^{-3}) complex. The Bande formation (2.81 g cm^{-3}) could to be the principal contributor to the subtle gravity high in the Anambra basin region. The interpreted vertical mafic intrusive (2.76 g cm^{-3}) that extends downwards from the base of the Cretaceous sedimentary cover to a depth of 10 km explains the prominent gravity high that culminates just east of Awka (Figs. 10, 12).

Two dominant trending magnetic lineaments (i.e., NE–SW and ENE–WSW) are interpreted in the lower Benue trough using high-resolution aeromagnetic data of the region (Abdullahi et al., 2019a). This is also supported by the present interpretation of the dominant NE–SW and ENE–WSW lineaments in the region. The NE–SW-oriented lineaments/faults are similar to the orientation of the Anambra basin, Abakaliki anticlinorium, and Afikpo syncline, and also to the orientation of the entire Benue trough (Abdullahi et al., 2019a; de Castro et al., 2012; Guiraud & Maurin, 1992).

The magnetic lineaments trending ENE–WSW are parallel to the ENE–WSW orientation of Pan-African basement faults and shear zones, e.g., Central African Shear Zone (CASZ) and dextral shear zone (Abdullahi et al., 2019a). The lineaments may have been developed as a result of the extensive of thermo-tectonic movements of the Pan-African plate relative to the South Atlantic Ocean and the Gulf of Guinea (Abdullahi et al., 2019a; Djomani et al., 1995; Torsvik et al., 2009).

Geologically, the anomaly encountered during the interpretation of the basement (i.e., magnetic and sedimentary basements) indicates that the region is complex with intrusions perhaps at different depths associated with weakly magnetic sources and basement uplift (SE end) and thickening (NW end) as a result of possibly high-density material in the lower half of the basin sequence. The calculated maps of the magnetic basement look very rugged with a good number of steep slopes coinciding with the magnetic lineaments, indicating fault control. The basement topography and lineaments (faults) may have a profound influence on structures developed within the overlying Cretaceous sedimentary sequence in that they may play a role in trapping hydrocarbons. Furthermore, the faults and associated brecciated fault zones may have provided suitable hosts for different kinds of economic mineralization such as barite, cadmium, coal, copper, gypsum, lead, silver, and zinc in the region (Abdullahi et al., 2019b).

5. Conclusions

Interpretation of the aeromagnetic and gravity data of the study region has provided maps of depth to the basement below the Cretaceous cover filling the lower Benue trough, and new insights into the basement architecture. The scaling spectral method, Euler method, and the SPI method were successful in the estimation of depths to the Precambrian magnetic basement using the aeromagnetic data in the region. Depths derived from the three different methods showed good mutual agreement. A gravity profile crossing the area is also modelled, yielding a 2D model. The basement depths estimated from both the magnetic and gravity data are greater than 8.0 km. The identified and mapped structural elements (lineaments) NE–SW, ENE–WSW, and WNW–ESE are closely associated with the trends of geological structures of the Pan-African plate which predated the compressional folds and faults within the Cretaceous sediments and strike-slip movements during the separation of Africa and South America.

Acknowledgements

We gratefully acknowledge the constructive comments of Prof. M.D. Thomas and the other anonymous reviewer and the Editor-in-Chief Prof. Pierre Keating. The comments have significantly improved the quality of the original submission.

References

Abdullahi, M., & Kumar, R. (2020). Curie depth estimated from high-resolution aeromagnetic data of parts of lower and middle Benue trough (Nigeria). *Acta Geodaetica Geophysica, 55*(4), 627–643.

Abdullahi, M., Kumar, R., & Singh, U. K. (2019b). Magnetic basement depth from high-resolution aeromagnetic data of parts of lower and middle Benue Trough (Nigeria) using scaling spectral method. *Journal of African Earth Sciences, 150*, 337–345.

Abdullahi, M., & Singh, U. K. (2018). Basement geology derived from gravity anomalies beneath the Benue Trough of Nigeria. *Arabian Journal of Geosciences, 11*, 694.

Abdullahi, M., Singh, U. K., & Roshan, R. (2019a). Mapping magnetic lineaments and subsurface basement beneath parts of Lower Benue Trough (LBT), Nigeria: Insights from integrating gravity, magnetic and geologic data. *Journal of Earth System Science, 128*, 17.

Adighije, C. (1981). A gravity interpretation of the Benue Trough, Nigeria. *Tectonophysics, 79*, 109–128.

Agagu, O. K., & Adighije, C. I. (1983). Tectonic and sedimentation framework of the lower Benue Trough, southeastern Nigeria. *Journal of African Earth Sciences, 1*(3/4), 267–274.

Ajayi, C. O., & Ajakaiye, D. E. (1981). The origin and peculiarities of the Nigerian Benue Trough: Another look from recent gravity data obtained from middle Benue. *Tectonophysics, 80*, 285–303.

Ajayi, C. O., & Ajakaiye, D. E. (1986). Structures deduced from gravity data in the middle Benue Trough, Nigeria. *Journal of African Earth Sciences, 5*, 359–369.

Ali, M. Y., Fairhead, J. D., Green, C. M., & Noufal, A. (2017). Basement structure of the United Arab Emirates derived from an analysis of regional gravity and aeromagnetic database. *Tectonophysics, 712–713*, 503–522.

Ali, M. Y., Watts, A. B., & Farid, A. (2014). Gravity anomalies of the United Arab Emirates: Implications for basement structures and infra-Cambrian salt distribution. *GeoArabia, 19*(1), 85–112.

Anudu, G. K., Stephenson, R. A., & Macdonald, D. I. M. (2014). Using high-resolution aeromagnetic data to recognize and map intra-sedimentary volcanic rocks and geological structures across the Cretaceous middle Benue Trough, Nigeria. *Journal of African Earth Sciences*, *99*(2), 625–635.

Bansal, A. R., & Dimri, V. P. (2010). Scaling spectral analysis: A new tool for interpretation of gravity and magnetic data. *Journal of Earth Science India, 3*(1), 54–68.

Blakely, R. J. (1996). *Potential Theory in Gravity and Magnetic Applications* (pp. 1–63). Cambridge University Press.

Carter, J. D., Barber, W., Tait, E. A., & Jones, G. P. (1963). The geology of parts of Adamawa, Bauchi and Bornu Provinces in northeastern Nigeria. *Bullettin of Geological Society of Nigeria, 30*, 109.

Cratchley, C. R., & Jones, G. P. (1965). An interpretation of the geology and gravity anomalies of the Benue Valley Nigeria. Oversea Geological Survey London, Geophysics paper no. 1.

de Castro, D. I., Bezerra, F. H. R., Sousa, M. O. I., & Fuck, R. A. (2012). Influence of Neoproterozoic tectonic fabric on the origin of the Potiguar Basin, northeastern Brazil and its links with West Africa based on gravity and magnetic data. *Journal of Geodynamics, 54*, 29–42.

Djomani, Y. H. P., Nnange, J. M., Diament, M., Ebinger, C. J., & Fairhead, J. D. (1995). Effective elastic thickness and crustal thickness variations in west central Africa inferred from gravity data. *Journal of Geophysical Research, 100*, 22047–22070.

Guiraud, R., & Maurin, J. C. (1992). Early Cretaceous rifts of western and central Africa. In P. A. Ziegler (Ed.) *Geodynamics of Rifting, Vol. 11. Case History Studies on Rifts: North and South America and Africa* (Vol. 213, pp. 153–168). Tectonophysics.

Hood, P. J. (1965). Gradient measurements in aeromagnetic surveying. *Geophysics, 30*, 891–902.

Jassen, M. E., Stephenson, R. A., & Cloetingh, S. (1995). Temporal and spatial correlations between changes in plate motions and evolution of rifted basins in Africa. *Bulletin of Geological Society of America, 107*(11), 1317–1332.

Keating, P. B. (1998). Weighted Euler deconvolution of gravity data. *Geophysics, 63*, 1595–1603.

King, L. C. (1950). Outline and disruption of Gondwanaland. *Geological Magazine, 87*, 353–359.

Kogbe, C. A. (1981). Attempt to correlate the stratigraphic sequence in the Middle Benue Basin with those of the Anambra and Upper Benue Basins. *Earth Evolution Science, 1*, 139–143.

Kumar, R., Bansal, A. R., Anand, S. P., Rao, V. K., & Singh, U. K. (2018). Mapping of magnetic basement in Central India from aeromagnetic data for scaling geology. *Geophysical Prospecting, 66*, 226–239.

Kumar, R., Bansal, A. R., & Ghods, A. (2020). Estimation of depths to bottom of magnetic sources using spectral methods: Application on Iran's aeromagnetic data. *Journal Geophysical Research, 125*, e2019JB018119.

Maluski, H., Coulon, C., Popoff, M., & Baudin, P. (1995). $^{40}Ar/^{39}Ar$ chronology, petrology and geodynamic setting of Mesozoic to early Cenozoic magmatism from the Benue Trough, Nigeria. *Journal of the Geological Society (London), 152*, 311–326.

Maus, S., & Dimri, V. P. (1996). Depth estimation from the scaling power spectrum of potential fields. *Geophysical Journal International, 124*, 113–120.

Mushayandebvu, M. F., van Driel, P., Reid, A. B., & Fairhead, J. D. (2001). Magnetic source parameters of two-dimensional structures using extended Euler deconvolution. *Geophysics, 66*, 814–823.

Nabighian, M. N., Grauch, V. J. S., Hansen, R. O., LaFehr, T. R., Li, Y., Peirce, J. W., Phillips, J. D., & Ruder, M. E. (2005). The historical development of the magnetic method in exploration. *Geophysics, 70*, 33ND-61ND.

Obaje, N. G. (2009). *Geology and Mineral Resources of Nigeria* (p. 221p). Springer.

Offodile, M. E. (1976). A review of the geology of the Cretaceous of the Benue Trough. In C. A. Kogbe (Ed.), *Geology of Nigeria* (pp. 31–330). Elizabethan Pub. Co.

Ofoegbu, C. O. (1984). Interpretation of aeromagnetic anomalies over Lower and Middle Benue Trough of Nigeria. *Geophysical Journal of Royal and Astronomical Society, 79*, 813–823.

Ofoegbu, C. O. (1985). Interpretation of an aeromagnetic profile across the Benue Trough of Nigeria. *Journal of African Earth Sciences, 3*(3), 293–296.

Ofoegbu, C. O., & Onuoha, K. M. (1991). Analysis of magnetic data over the Abakaliki Anticlinorium of the Lower Benue Trough, Nigeria. *Marine and Petroleum Geology, 8*, 174–183.

Ogungbesan, G. O., & Adedosu, T. A. (2019). Geochemical record for the depositional condition and petroleum potential of the late cretaceous mamu formation in the western flank of anambra basin. *Green Energy and Environment*. https://doi.org/10.1016/j.gee.2019.01.008.

Ogunmola, J. K., Ayolabi, E. A., & Olobaniyi, S. B. (2016). Structural-depth analysis of the Yola Arm of the Upper Benue Trough of Nigeria using high resolution aeromagnetic data. *Journal of African Earth Sciences, 124*, 32–43.

Ojoh, K. A. (1992). The Southern part of the Benue Trough (Nigeria) Cretaceous stratigraphy, basin analysis, paleo-oceanography and geodynamic evolution in the equatorial domain of the South Atlantic. *NAPE Bullettin, 7*, 131–152.

Onwuemesi, A. G. (1997). One-dimensional spectral analysis of aeromagnetic anomalies and curie depth isotherm in the Anambra basin of Nigeria. *Journal of Geodynamics, 23*(2), 95–107.

Philips, J. D., Hansen, R. O., & Blakely, R. J. (2007). The use of curvature in potential-field interpretation. *Exploration Geophysics, 38*, 111–119.

Pilkington, M., & Todoeschuck, J. P. (1993). Fractal magnetization of continental crust. *Geophysical Research Letters, 2*, 627–630.

Rao, C. V., Chakravarthi, V., & Raju, M. L. (1993). Parabolic density functions in sedimentary basin modeling. *Pure and Applied Geophysics, 140*(3), 493–501.

Ravat, D. (1996). Analysis of the Euler method and its applicability in environmental magnetic investigations. *Journal of Environmental and Engineering Geophysics, 1*, 217–219.

Reford, S. W., & Paterson, J. M. (2010). Nigeria' Nationwide High-resolution Airborne Geophysical Surveys. SEG Annual Meeting, Denver Extended Abstract.

Reid, A. B. (1995). *Euler deconvolution: past, present, and future: a review* (pp. 272–273). Tulsa: Extended abstract of the 65th Annual Meeting of the Society of Exploration Geophysics.

Reid, A. B., Allsop, J. M., Granser, H., Miliett, A. J., & Somerton, W. I. (1990). Magnetic interpretations in three dimensions using Euler deconvolution. *Geophysics, 55*, 80–91.

Reid, A. B., & Thurston, J. B. (2014). The structural index in gravity and magnetic interpretation: Errors, uses, and abuses. *Geophysics, 79*(4), J61–J66.

Salem, A., Green, C., Cheyney, S., & Fairhead, J. D. (2014). Mapping the depth to magnetic basement using inversion of pseudogravity: Application to the Bishop model and the Stord Basin, northern North Sea. *Interpretation, 2*, T69–T78.

Salem, A., & Smith, R. (2005). Depth and structural index from the normalized local wavenumber of 2D magnetic anomalies. *Geophysical Prospecting, 53*, 83–89.

Spector, A., & Grant, F. S. (1970). Statistical model for interpreting aeromagnetic data. *Geophysics, 35*, 293–302.

Talwani, M., Worzel, J., & Ladisman, M. (1959). Rapid gravity computations for two dimensional bodies with application to the Mendocino submarine fracture zone. *Journal of Geophysical Research, 4*(1), 49–59.

Telford, W. M., Geldart, L. P., & Sheriff, R. E. (1998). *Applied Geophysics* (2nd ed., p. 770). Springer.

Thompson, D. T. T. (1982). Euler, a new technique for making computer assisted estimates from magnetic data. *Geophysics, 47*, 31–37.

Thurston, J. B., & Smith, R. S. (1997). Automatic conversion of magnetic data to depth, dip, susceptibility contrast using the SPITM method. *Geophysics, 62*, 807–813.

Tokam, K. A. P., Tabod, C. T., Nyblade, A. A., & Julià, J. (2010). Structure of the crust beneath Cameroon, West Africa, from the joint inversion of Rayleigh wave group velocities and receiver functions. *Geophysical Journal International, 183*, 1061–1076.

Torsvik, T. H., Rousse, S., Labails, C., & Smethurst, M. A. (2009). A new scheme for the opening of the South Atlantic Ocean and the dissection of an Aptian salt basin. *Geophysical Journal International, 177*, 1315–1333.

Uzuakpunwa, A. B. (1974). The Abakaliki pyroclastics, Eastern Nigeria, new age and tectonic implications. *Geological Magazine, 111*, 65–70.

Won, I. J., & Bevis, M. (1987). Computing the gravitational and magnetic anomalies due to a polygon: Algorithms and FORTRAN subroutines. *Geophysics, 52*, 232–238.

(Received June 25, 2020, revised June 15, 2021, accepted June 18, 2021)